Life cycle assessment of nanocellulose-reinforced advanced fibre composites

CrossMark

Martin Hervy [1], Sara Evangelisti, Paola Lettieri[*], Koon-Yang Lee[*, 1]

Department of Chemical Engineering, University College London, Torrington Place, WC1E 7JE, London, United Kingdom

ARTICLE INFO

ABSTRACT

The research and development of nanocellulose-reinforced polymer composites have dramatically increased in recent years due to the possibility of exploiting the high tensile stiffness and strength of nanocellulose. In the work, the environmental impact of bacterial cellulose (BC)- and nanofibrillated cellulose (NFC)-reinforced epoxy composites were evaluated using life cycle assessment (LCA). Neat polylactide (PLA) and 30 wt.-% randomly oriented glass fibre-reinforced polypropylene (GF/PP) composites were used as benchmark materials for comparison. Our cradle-to-gate LCA showed that BC- and NFC-reinforced epoxy composites have higher global warming potential (GWP) and abiotic depletion potential of fossil fuels (ADf) compared to neat PLA and GF/PP even though the specific tensile moduli of the nanocellulose-reinforced epoxy composites were higher than neat PLA and GF/PP. However, when the use phase and the end-of-life of nanocellulose-reinforced epoxy composites were considered, the "green credentials" of nanocellulose-reinforced epoxy composites were comparable to that of neat PLA and GF/PP composites. Our life cycle scenario analysis further showed that the cradle-to-grave GWP and ADf of BC- and NFC-reinforced epoxy composites could be lower than neat PLA when the composites contains more than 60 vol.-% nanocellulose. This suggests that nanocellulose-reinforced epoxy composites with high nanocellulose loading is desirable to produce materials with "greener credentials" than the best performing commercially available bio-derived polymers.

1. Introduction

The growing awareness on the consequences of depletion of fossil resources and the increasing demand for more environmental friendlier products have led to the development of sustainable and/or renewable composites to replace petroleum-derived plastics [1], particularly in the automotive industry [2]. In this context, nanometre-scale cellulose fibres, or nanocellulose, are emerging green nano-reinforcements for polymers [3]. The major driver for utilising nanocellulose as reinforcement for polymer is the possibility of exploiting the high tensile stiffness and strength of the cellulose crystals [4]. Theoretical predictions [5–7] and numerical simulations [8–10] estimated the tensile moduli of single cellulose crystal to be between 58 and 180 GPa. X-ray diffraction [11–13] and

Raman spectroscopy [14–16] further showed experimentally that a single cellulose nanofibre possess tensile moduli of between 100 and 160 GPa. The tensile strength of a single cellulose crystal has also been estimated theoretically to be between 0.3 and 22 GPa [17–20]. The high tensile modulus and strength of nanocellulose fibres suggest that they could potentially serve as replacement for glass fibres given their low toxicity and low density (1.5 g cm^{-3} for nanocellulose versus 2.5 g cm^{-3} for glass fibres). As a result, numerous research effort has been poured into the use of nanocellulose as reinforcement for polymers [21,22].

Nanocellulose can be produced via two approaches: top-down and bottom-up. In the top-down approach, (ligno)cellulosic biomass, such as wood fibres, is disintegrated into nanofibres. The earliest report on the preparation of wood-derived nanocellulose from (ligno)cellulosic biomass was presented by Wurhmann et al. [23]. The authors disintegrated ramie, hemp and cotton fibres using high intensity ultrasound into their respective elementary fibrils with diameters as small as 6 nm. Later, Herrick et al. [24] and Turbak et al. [25] used high pressure homogenisers to reduce the diameter of wood pulp to 10 nm. Wood-derived nanocellulose,

herein termed nanofibrillated cellulose (NFC), can also be produced using stone grinders [26], whereby the high shearing forces generated by the static and rotating grinding stones fibrillates micrometre-sized pulp fibres into cellulose nanofibres. The bottom-up approach, on the other hand, utilises the fermentation of low molecular weight sugars using cellulose-producing bacteria, such as from the *Acetobacter* species, to synthesise nanocellulose [27]. Nanocellulose synthesised by bacteria, herein termed bacterial cellulose (BC), is pure cellulose without impurities that are typically present in wood-derived nanocellulose, such as hemicellulose, pectin and traces of lignin. In addition to this, both BC and NFC possess cellulose-I structure [28]. Even though BC possesses higher degree of crystallinity compared to NFC (72% for BC and 41% for NFC, respectively, based on area under the X-ray diffraction spectra), both BC and NFC were found to possess similar reinforcing ability for polymers [29].

The first use of nanocellulose as reinforcement in polymers, namely polypropylene, polystyrene and polyethylene, was reported by Boldizar et al. [30]. The authors found that the tensile modulus increased from 2.4 GPa for neat polystyrene to 5.2 GPa for polystyrene reinforced with 40 wt.-% NFC. Yano et al. [31] reported tensile modulus and strength of up to 20 GPa and 325 MPa, respectively, for BC-reinforced epoxy composites containing 65 wt.-% BC loading. Tensile modulus and strength of up to 8 GPa and 202 MPa, respectively, have also been obtained for NFC-reinforced hydroxyethyl cellulose composites containing 68 wt.-% NFC loading [32]. It is therefore evident that high performance BC- and NFC-reinforced polymer composites can be produced. However, one major question still remains: "*Are nanocellulose-reinforced polymer composites truly environmentally friendly compared to commercially available renewable polymers or engineering materials?*" Li et al. [33] recently used life cycle assessment (LCA) to analyse the environmental impact associated with the production of NFC using high pressure homogenisation and high intensity sonication. TEMPO-oxidised and chloroacetic acid-etherified kraft pulp were chosen as the starting materials in their LCA model. The authors found that NFC produced from high-pressure homogenisation of TEMPO-oxidised kraft pulp has the lowest environmental impact among all the NFC production routes studied. In a recent LCA study conducted by Hohenthal et al. [34], the non-renewable energy consumption associated with the production of NFC nanopaper was estimated to be 107.5 MJ kg^{-1}. This is significantly higher than the energy consumed for the production of polylactide (PLA), which is estimated to consume only 42 MJ kg^{-1} [35] of energy.

With increasing demand for environmental friendlier materials, it is timely to investigate the environmental impact associated with the manufacturing of nanocellulose-reinforced polymer composites. Therefore in this work, we quantify the environmental impact associated with the manufacturing of BC- and NFC-reinforced polymer composites through a life cycle assessment approach, starting from the production of nanocellulose (i.e. the cradle) to the end-of-life (i.e. the grave) of the nanocellulose-reinforced polymer composites. Joshi et al. [36] have suggested that natural fibre composites could potentially compete environmentally with glass fibre-reinforced polymer composites in most applications. In this work, a comparison of environmental impact between BC-/NFC-reinforced polymer composites and glass fibre-reinforced polymer composites is also reported.

2. Methodology

LCA is the internationally recognised method used to assess of the environmental performance of a product. ISO 14040:2006 (E) states that LCA should "*consider the entire life cycle of a product from raw material extraction and acquisition, through energy and material production and manufacturing, to use and end-of-life treatment and final disposal*". Any LCA study should start with a carefully defined scope of the study, functional unit and system boundaries. These elements are the guideline that will help reaching a conclusion that answers the initial objective of the LCA; whether it is the comparison of different products or the identification of a "hotspot". Following this step, a life cycle inventory (LCI) consisting of the materials and energy used in every step of the life cycle is compiled. Using this LCI, life cycle impact assessment (LCIA) can then be conducted. All the inputs and outputs of the system are allocated to the different environmental impact categories. Finally, the outcome of the LCA can be given in the form of interpretations and recommendations to lower the environmental burden of the system [37].

2.1. Goal and scope definitions

The aim of this study is to evaluate the environmental impact of high performance BC- and NFC-reinforced epoxy composites through a cradle-to-grave LCA including their manufacturing, use phase and end-of-life. Two commercially available benchmark materials were chosen for comparison: (i) 30 wt.-% randomly oriented glass fibre-reinforced polypropylene (GF/PP) composites and (ii) polylactide, which is considered the best performing bio-derived polymer [3]. The system boundary for our nanocellulose-reinforced epoxy composites and our benchmark materials is shown schematically in Fig. 1. A distinction is made between the foreground system, which is defined as the processes of main importance in regards to the study (direct measurements can often be taken), and the background system, which is defined as the processes used to support the foreground system (supply of energy and materials) [38].

2.2. Description of the polymer and composite manufacturing processes

The manufacturing of BC- and NFC-reinforced epoxy composites modelled in our system is based on our previous work [29]. This study was chosen as high loading of nanocellulose, a pre-requisite to producing high performance nanocellulose-reinforced polymer composites [3], was achieved using conventional vacuum assisted resin infusion (VARI), a widely used composite manufacturing technique. Briefly, never-dried bleached birch kraft pulp (*Betula pendula*) was passed through a Supermass Colloider (Masuko Sangyo Co., Kawaguchi, Japan) seven times and the final obtained consistency of NFC in water was approximately 2 wt.-%. The NFC suspension was diluted to 0.4 wt.-% prior to nanopaper manufacturing. Similarly, BC pellicles were first cut into small pieces and blended (Breville BL18 glass jug blender, Pulse Home Products Ltd., Oldham, UK) for 2 min at a consistency of 0.1 wt.-%. The manufacturing of both BC and NFC nanopaper closely resembles that of conventional paper manufacturing process, whereby the BC and NFC suspension were vacuum filtered, wet pressing under a 10 kg weight, followed by drying at 55 °C to obtain BC and NFC nanopapers. To manufacture BC- and NFC-reinforced epoxy composites, 11 nanopapers were sandwiched between two PTFE coated glass fabrics (FF03PM, Aerovac, West Yorkshire, UK) and placed on top of a polyester porous flow medium (15087B, Newbury Engineer Textile, Berkshire, UK). Another polyester porous flow medium was placed on top of the PTFE coated glass fabric. A heat stabilised Nylon 6 vacuum bag (Capran 519, Aerovac, West Yorkshire, UK) was then used to cover the whole set up and vacuum sealant tape (SM5127, Aerovac, West Yorkshire, UK) was used to seal the set up. A vacuum was then applied (~15 mmHg) and the liquid epoxy resin (PRIME 20ULV, Gurit Ltd, Isle of Wight and Hamble, UK) was fed at room temperature from the bottom of the
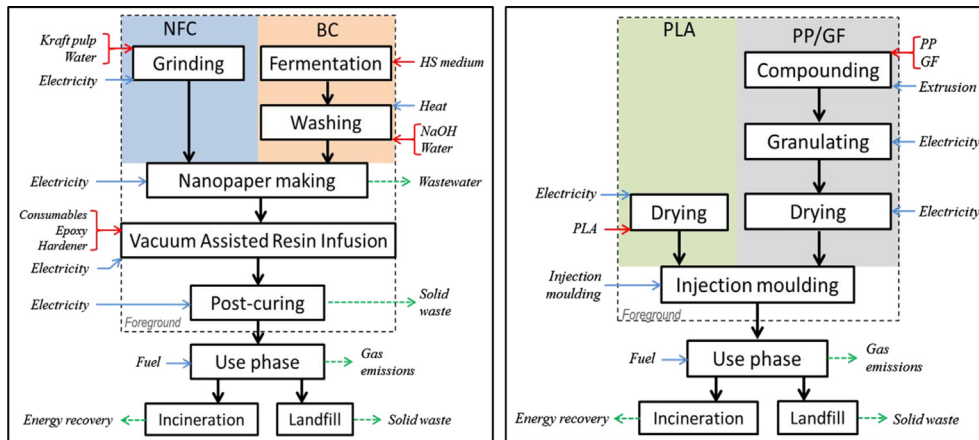
Fig. 1. Schematic diagram showing the system boundaries of the model representing the life cycle of BC- and NFC-reinforced polymer composites (left), and PLA and GF/PP composite (right). The red, blue and green arrows represent consumables or raw materials required, energy input and waste (materials and energy), respectively. (For interpretation of the references to colour in this figure legend, the reader is referred to the web version of this article.)

flow medium (tooling side) through the stack of nanopapers and exit through non-tooling side. The resin was left to cure at room temperature for 24 h, followed by a post-curing step at 50 °C for 16 h. The resulting BC- and NFC-reinforced epoxy composite panels were ~1 mm thick, containing 49 vol.-% and 58 vol.-% of BC and NFC loadings, respectively. In our LCA model, we modelled the tensile properties of commercially available randomly oriented GF/PP composite consisting of 30 wt.-% glass fibres,[2] under the trade name of Eurostar Starpylen MX06050.[3] To manufacture the GF/PP composites, the glass fibres were assumed to be compounded with polypropylene in an extruder prior to pelletisation and injection moulded into the final composite parts. To manufacture neat PLA parts, our model assumed that dried PLA pellets were injection moulded to produce the final PLA part.

2.3. Functional unit

A functional unit (f.u.) quantifies the function provided by the analysed system and provides a base for comparison with alternative systems. In order to compare our four different materials with different mechanical performances, a performance indicator based on the specific tensile stiffness of the materials was used to calculate the equivalent mass of the material required to reach the same level of performance [39]. The equivalent mass of material required is expressed as:

$$\frac{m - m_{ref}}{m_{ref}} = \frac{E_{ref} / \rho_{ref}}{E / \rho} - 1 \tag{1}$$

where m, E, ρ are the mass, tensile modulus and density of BC-reinforced epoxy composites, GF/PP model composites and neat PLA, respectively. m_{ref}, E_{ref} and ρ_{ref} are the mass, tensile stiffness and density of a reference material. In our LCA model, m_{ref} = 1 kg of NFC-reinforced epoxy composite was arbitrarily chosen as our reference. The derivation of Equation (1) can be found in the Appendix A. The mass of materials compared in this LCA model along with materials properties are summarised in Table 1.

---

[2] This corresponds to a glass fibre volume fraction of ~14 vol.-%.
[3] Mechanical data obtained from http://www.matweb.com/.

2.4. Calculation method and impact categories

Our LCA model uses the CML 2001 impact assessment method (April 2013 version) developed by the Centre for Environmental Science in Leiden University [40] using a life cycle engineering software, GaBi (version 6, PE International, Leinfelden-Echterdingen, Germany). This method uses midpoint indicators to model the effects of substances on the environment at an early stage (also known as problem-oriented approach), which minimises uncertainties [41]. The chosen impact indicators for this LCA study along with their brief description are summarised in Table 2. These impact categories have been chosen based on their significance to this LCA model and their link to distinct environmental mechanisms.

2.5. Key assumptions

The following assumptions were made in our LCA model:

(i) The yield of BC is highly dependent on the strain of cellulose-producing bacteria used, the carbon source, supplement supplied and the culture time [27]. In our LCA model, BC is assumed to be produced by *A. xylinum* (ATCC 53582) using Hestrin-Schramm medium [42] consisting of 2% (w/v) glucose, 0.5% (w/v) yeast extract and peptone, 0.27% (w/v) disodium hydrogen phosphate and 0.115% (w/v) citric acid. The BC yield used in our LCA model was 3.2 g L^{-1} based on our in-house preliminary study.

(ii) BC is purified by heating the BC pellicles in 0.1 M NaOH solution to 80 °C for 20 min. In our LCA model, we assumed that 36 L of 0.1 M NaOH solution is needed to purify 653 g (dry weight) of BC pellicles.

(iii) The manufacturing of nanocellulose-reinforced composite panels will no doubt require more epoxy resin than what was needed by the final BC- and NFC-reinforced composite panels as additional epoxy resin was needed to fill the gap in the vacuum bag and infusion tubes. Nevertheless, we assumed in this LCA model that the additional epoxy resin needed exert no significant influence on the LCA results.

(iv) Material losses during kraft pulp grinding, nanopaper manufacturing, polymer and glass fibres compounding, injection moulding and (composite) parts finishing were assumed to be negligible. Heat loss during the post curing of

Table 1
The functional unit used in this LCA study. E, ρ and m denote the tensile modulus, density and equivalent mass of the materials required. E and ρ of BC- and NFC-reinforced epoxy composites, as well as neat PLA were obtained from Lee et al. [29] and Montrikittiphant et al. [60], respectively.

Material	E (GPa)	ρ (kg m^{-3})	E/ρ (GPa m^3 kg^{-1})	m(total) (kg)	m(reinforcement) (kg)
PLA	3.9 ± 0.2	1210	3.22	1.96	0
GF/PP[a]	5.7	1120	5.09	1.24	0.392
NFC/epoxy	8.5 ± 0.2	1350	6.30	1.00	0.650
BC/epoxy	7.1 ± 0.1	1320	5.38	1.17	0.653

[a] The properties used in this study are based on commercially available randomly oriented GF/PP composites under the trade name of Eurostar Starpylen MX06050.

the BC- and NFC-reinforced epoxy composites was assumed to be insignificant.

(v) A recent study by Josset et al. [43] showed that an energy requirement of 5.25 kWh kg^{-1} was needed to fibrillate kraft pulp to NFC using a Masuko grinder. This value was used in our LCA model for the production of NFC from kraft pulp.

(vi) An industrial paper manufacturing process was modelled in our life cycle engineering software, GaBi, to model the manufacturing of BC and NFC nanopapers.

(vii) The environmental impacts associated with the transportation of materials were neglected.

(viii) The efficiency of all electrical appliances (vacuum oven, resin infusion plates, vacuum pumps etc) was assumed to be 100%.

(ix) BC- and NFC-reinforced epoxy composites, GF/PP and PLA were assumed to be equally durable in our LCA model.

2.6. Life cycle inventory (LCI)

All the data used in this study was obtained from: (i) the GaBi databases, (ii) Ecoinvent version 2.2, (iii) literature values and (iv) our own estimations. Detailed inventory can be found in Appendix B.

2.6.1. Foreground data

All the input and output data were scaled to the equivalent of manufacturing the previously calculated mass of materials to be compared. The electricity usage of the vacuum pump was measured using P4400 Kill-A-Watt power usage meter (P3 International, New York, USA).

2.6.2. Background data

The electricity production was assumed to be supplied from the electricity grid mix for Great Britain (45.9% from natural gas, 28.3% from hard coal, 16.3% from nuclear, 1.3% from heavy fuel oil, 0.3% from coal gases and 8% from renewable energies). Global and European data averages were used in the absence of data from Great Britain. If data was not available from both Great Britain and Global/

European averages, the data from Switzerland or Germany was then used.

2.6.3. Energy balance

To estimate the energy required in any process steps, the following equation was used:

$$Q = \int_{T_1}^{T_2} \left(\sum_i m_i \times C_{P,i} \right) dT \tag{2}$$

where Q is the energy required, T_1 and T_2 are the initial and final temperatures, m_i and $C_{P,i}$ are the mass and the heat capacity of compound i, respectively. For the estimation of the energy required to post cure BC- and NFC-reinforced epoxy composites, the heat capacities of cellulose and epoxy resin were taken as 1.55 J g^{-1} K^{-1} [44] and 1 J g^{-1} K^{-1} [45], respectively. The energy required to heat the water for the purification of BC pellicles was also calculated using Equation (2).

2.7. Use phase and end-of-life

A cradle-to-grave LCA was performed in this study, whereby the use phase of the polymer and composite parts in a car (a highly researched application for green composites) [2] and their end-of-life were considered in a hypothetical scenario.

2.7.1. Use phase impact

To evaluate the environmental impact associated with the use phase of the polymer and composite parts in a car, the fuel consumption was allocated as a function of the weight of the parts in the car using [46]:

$$\text{Fuel economy of the panel} = \frac{\text{Weight of the panel}}{\text{Weight of the car}}$$
$$\times \text{Fuel economy of the car} \times c \tag{3}$$

Table 2
The impact categories used in this LCA study and their brief description.

Impact indicators (unit)	Description
GWP (Global warming potential, in CO_2 eq)	This takes into accounts the emissions of gas that will contribute to the greenhouse effects (heating effect due to the exposition of gases to sunrays) such as CO_2, CH_4, N_2O and CFCs.
AP (Acidification potential, in SO_2 eq)	The emissions of SO_2, NO_X and NH_3 are responsible for the general acidification of soils and waters that ultimately leads to less available nutrients for plants.
ADf (Abiotic depletion potential - fossil fuel, in MJ)	This impact only accounts for the energy consumption linked to non-renewable fossil resources. It is only a part of the CED (cumulative energy demand)
POCP (Photochemical ozone creation potential, in ethene eq)	Related to the catalyst effect of the VOC to form NO_2. Ozone creation has a negative impact on both human health and ecosystems.
FETP (Freshwater ecotoxicity potential, in DCB eq)	Measured in dichlorobenzene equivalent. Important in systems using large amounts of water that can become contaminated by chemicals.

A factor "c" was introduced to account for aerodynamics, as the reduction in fuel consumption of the polymer and composite parts is not only directly proportional to the weight reduction of the car [46]. A c value of 0.5, which signifies that a 10% weight reduction of the car lowers the fuel consumption by 5%, was chosen according to a study conducted on Peugeot - Citroën cars [47]. The equivalent distance used to model the use phase of each part was calculated based on an average car weighing 1500 kg driven for 200,000 km with a fuel consumption of 7.3 L km^{-1}. This fuel consumption also corroborated the average fuel consumption of a car in the EcoInvent database.

2.7.2. End-of-life (EOL)

In 2011, it was estimated that 50% of the plastic waste generated in Switzerland went into landfills, 30% of the plastic waste were incinerated to recover energy whilst the remainder were recycled [48]. The process of recycling depends on numerous factors such as waste flow and the type of plastic. Due to the uncertainty associated with the recycling process, our LCA model assumed that 60% of composite panels would go into landfill and 40% of our composite panels were incinerated to recover energy. The process of recycling was not considered in our LCA model. All the glass fibres in GF/PP were assumed to be incombustible and sent to landfill as part of the combined ash from the incinerator. Furthermore, a recent report published by the European Plastics Recyclers Association showed that less than 15% of polymer waste from the automotive industry is recycled [49], with approximately 60% of these waste disposed in landfill or incinerated without energy recovery. Therefore, our LCA assumed that 60% of PLA was sent to landfill and 40% incinerated to recover energy. A recent study on the anaerobic digestion of PLA in landfills showed that no statistically significant biogas (CH$_4$ and CO$_2$) was generated [50]. Therefore, our LCA model further assumed that there was no significant biogas contribution when PLA was landfilled compared to our other materials.

3. Results and discussion

3.1. Cradle-to-gate analysis

A cradle–to-gate LCA model includes all steps from raw materials extraction to the finished product at the factory gate. The cradle-to-gate GWP and ADf associated with the production of PLA, GF/PP, BC- and NFC-reinforced epoxy composites are shown in Fig. 2. Even though the equivalent mass of neat PLA is larger, the GWP of neat PLA is lower than GF/PP. This could be attributed to the 1.9 kg CO$_2$ eq kg^{-1} of environmental credits of PLA as a result of carbon sequestration associated with corn production [35], whereby for 1 kg of PLA, 2.5 kg of corn is needed.[4] The ADf for PLA however, is higher than that of GF/PP. As GF/PP possess higher tensile modulus compared to PLA (5.7 GPa vs 3.9 GPa), the equivalent mass of GF/PP required would be much smaller than that of PLA to sustain the same tensile load, leading to the observed lower environmental impact of GF/PP in other impact categories (see Appendix C for a comprehensive environmental impact of all modelled materials). Nevertheless, both BC- and NFC-reinforced epoxy composites have higher environmental impact compared to our benchmark PLA and GF/PP. The results showed that the GWP of both BC- and NFC-reinforced epoxy composites are higher than that of PLA and GF/PP. Furthermore, the ADf of the production of BC-reinforced epoxy composites was found to be 2.4 and 2.6 times higher than neat PLA and GF/PP (see Fig. 2), respectively, even though BC-reinforced epoxy composites possess higher tensile
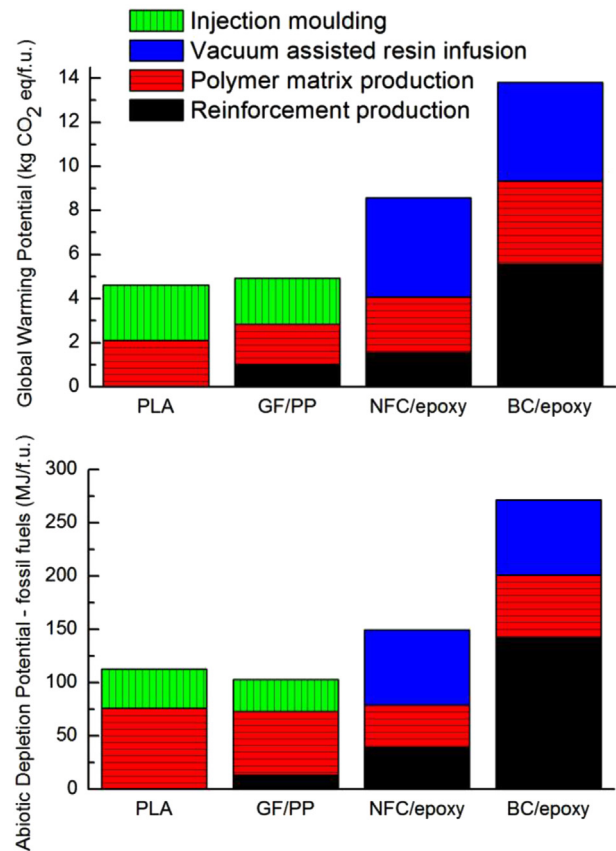
Fig. 2. Global warming potential and fossil energy consumption for the production (from cradle-to-gate) of our two benchmark materials and two nanocellulose-reinforced composites.

modulus compared to neat PLA and GF/PP, implying that we need less BC-reinforced epoxy composites to comply with the functional unit. Similar observations could also be made for NFC-reinforced epoxy composite, whereby higher ADf is observed for the manufacturing these composites compared to neat PLA and GF/PP. The higher GWP and ADf associated with the manufacturing of BC- and NFC-reinforced epoxy composites suggest that nanocellulose-reinforced polymer composites might not be environmental friendlier than commercially available bio-derived polymer, such as PLA or engineering materials, such as GF/PP composites.

From Fig. 2, it can be seen that one of the major contributors to the environment is the manufacturing of BC- and NFC-reinforced epoxy composites using VARI. This is due to the consumables used in the manufacturing processes, many of which are not eco-friendly. Table 3 further shows the contributions of the consumables used in the VARI process to the environment. These

Table 3
Detailed impacts associated with the production of the BC- and NFC-reinforced epoxy composites.

Consumables used	GWP (kg CO$_2$ eq/f.u.)	ADf (MJ/f.u.)
Resin feed tube	0.07	1.96
Porous medium	1.30	33.66
Sealants	0.41	11.38
Vacuum bag	0.55	6.29
Consumables end-of-life	0.30	−4.48

consumables constitute to approximately 24% and 45% of the total ADf associated with the VARI process of BC- and NFC-reinforced epoxy composites, respectively. The production of the porous flow medium used in the VARI, for example, has almost as high ADf as the production of the epoxy resin used. Furthermore, it can also be seen from Fig. 2 that the GWP and ADf for the production of BC- and NFC-reinforced epoxy composites stems from the production of the reinforcing phase, i.e. the production NFC from wood pulp and the biosynthesis of BC from low molecular weight sugars. It should also be noted that the equivalent mass of glass fibres, NFC and BC considered in this study are different (see Table 1). Therefore, the higher GWP and ADf for the production of NFC can be attributed to the larger amount of NFC required to reinforce the epoxy matrix (versus the amount of GF required in the PP). Nonetheless, it is clear that the production process of BC is much more energy intensive, leading to higher ADf compared to the production of NFC and GF, even when the differences in the mass of NFC and GF are considered. This is due to the energy required to produce the chemicals used for the HS medium.

To further elucidate this, a detailed hot spot analysis of the relative environmental impacts associated with the synthesis of BC is shown Fig. 3. The production of the glucose used for the HS medium (4.08 kg per functional unit) contributes 61 MJ in the ADf category. This accounts for half of the ADf in the production of 0.653 kg of BC (131 MJ) and accounts for 25% of the ADf in production of 1.17 kg of BC-reinforced epoxy composites (272 MJ). Nevertheless, the production of glucose also provides an environmental credit in the GWP indicator as glucose is produced from starch, which is in turn obtained from corn cultivation where carbon dioxide can be sequestered. In addition to this, the use of disodium phosphate in HS medium is also a major contributor to the acidification potential and freshwater ecotoxicity potential of the BC-reinforced epoxy composite (see Appendix C for detailed breakdown of every impact indicator) accounting for respectively 21% and 37% of these impacts. The environmental burden associated with BC production also originates from the purification of BC after culturing in HS medium. The cultured BC pellicles have to be washed and purified to remove any chemicals and bacteria used in HS medium as highly purified BC pellicles possess better thermal stability, thermo-mechanical and mechanical properties [51–53]. Our LCA model results show that this purification step, equivalent to 2.6 kg CO_2 eq, corresponding to 54% and 19%, respectively of the GWP of the BC production (see Fig. 3) and the manufacturing of BC-reinforced epoxy composite. In terms of ADf, the 22.7 MJ required for the purification corresponds to 17% of the BC production.
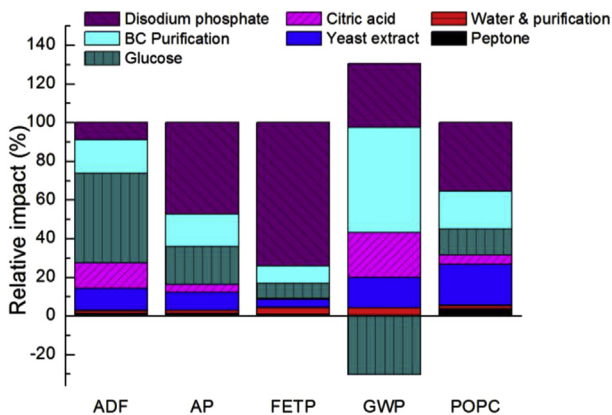
3.2. Cradle-to-grave study

A major contributor to the life cycle global warming potential is the use phase associated with the composite automotive part [54,55] The heavier the part, the higher the fuel consumption contributed by the part and thus, more exhaust gas is produced. As aforementioned, the motivation of using nanocellulose as reinforcement for polymers is the possibility of exploiting the high tensile stiffness and strength of cellulose crystals [56], thereby producing high performance lightweight structures, reducing fuel consumption of the vehicle. The GWP and ADf associated with the manufacturing, use phase and end of life of PLA and the other composites in our cradle-to-grave scenario is shown in Fig. 4. Contrary to the cradle-to-gate results, which show that the environmental burden associated with the manufacturing of BC- and NFC-reinforced epoxy composites was higher compared to the production of GF/PP and neat PLA, the cradle-to-grave LCA study showed otherwise. When the use phase of the polymer/composite parts was considered, neat PLA contributes the highest cradle-to-grave GWP and ADf. On the other hand, GF/PP composites contributed the lowest cradle-to-grave GWP and ADf compared to the neat PLA. This can be attributed to the differences in the mass required between the two materials to reach the same performance (see Table 1). Conversely, even though the equivalent mass of GF/PP was higher than that of BC- and NFC-reinforced epoxy composites, the GWP and ADf for the manufacturing of GF/PP composites were lower than that of the nanocellulose-reinforced epoxy composites, leading to lower cradle-to-grave GWP and ADf compared to our
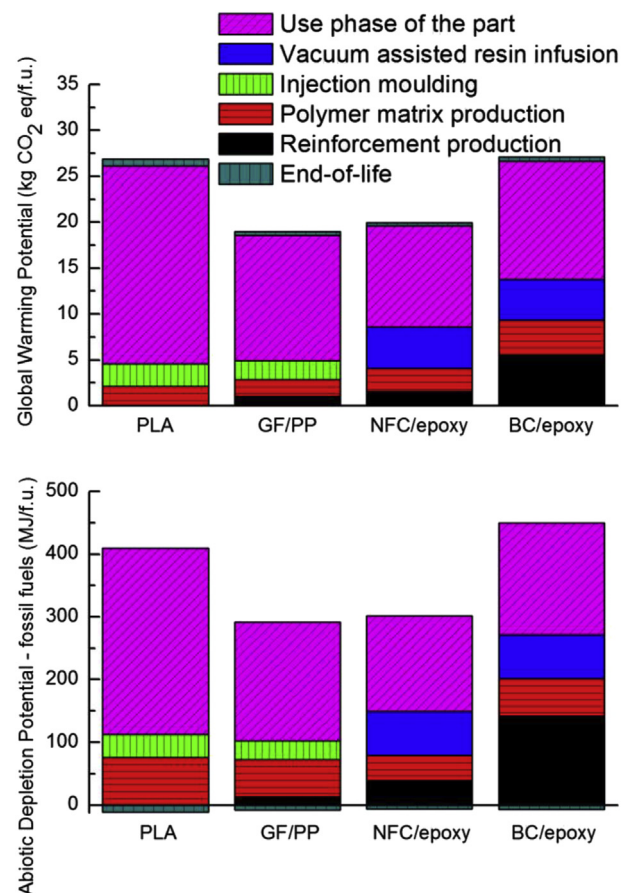
Fig. 4. GWP and ADf (from cradle-to-grave) of our two benchmark materials and two nanocellulose-reinforced composites.

Fig. 3. Detailed hot spot analysis of the production of bacterial cellulose.

model nanocellulose-reinforced epoxy composites. Our LCA model suggests that whilst the manufacturing of nanocellulose-reinforced epoxy composites might not be as environmentally friendly as neat PLA and GF/PP, the "green credentials" of nanocellulose-reinforced epoxy composites are comparable to that of neat PLA and GF/PP composites when the use phase and end-of-life of the composites were considered.

A recent study by Pietrini et al. [57] showed that the non-renewable energy use for the manufacturing of nanoclay-reinforced polymer composites was a function of the tensile modulus of the nanocomposites. Lee et al. [3] have also recently showed that the tensile modulus ($E_{composites}$) of nanocellulose-reinforced polymer composites can be predicted using simple rule-of-mixture (see Equation (4)) based on the tensile moduli of the cellulose nanopaper (E_f), the matrix (E_m) and the loading fraction of nanocellulose (v_f), respectively. This is due difficulties in impregnating a high v_f nanocellulose network with monomers or polymers at a single fibre level [3], hypothesised to be due to the tendency of nanocellulose to form strong hydrogen bonds between adjacent fibrils producing a dense cellulose network, which is difficult to impregnate. Furthermore, the effective moduli of single nanocellulose fibre in the network were estimated to be as low as ~30 GPa [58]. This leads to an estimated tensile modulus of cellulose nanopapers of ~10 GPa, $1/3$ of the effective tensile modulus of the cellulose nanofibres [59]. This value is consistent with our previous work [29,60].

$$E_{Composites} = v_f E_f + \left(1 - v_f\right) E_m \qquad (4)$$

In order to identify the v_f at which BC- and NFC-reinforced epoxy composites will perform environmentally better compared to neat PLA and GF/PP, we have plotted the cradle-to-grave GWP and ADf of BC- and NFC-reinforced epoxy composites as a function of v_f using $E_{composites}$ calculated[5] from Equation (4) (see Fig. 5). As a comparison, the cradle-to-grave GWP and ADf for neat PLA and 30 wt.-% randomly oriented GF/PP composites are also shown on the same figure. The dotted line shown in Fig. 5 represents an hypothetical state whereby cellulose nanopapers can be used to reinforce polymer matrices at such extreme fibre loadings. Our analysis showed that with increasing v_f, whereby the production of both NFC and BC will place heavier environmental burden, the cradle-to-grave GWP and ADf decreased. This is due to the increase of the tensile moduli of BC- and NFC-reinforced epoxy composites, thereby lowering the amount of materials required to comply with the functional unit and reducing the impact of the use phase significantly. Whilst both the cradle-to-grave GWP and ADf for BC- and NFC-reinforced epoxy composites can be lower than that of neat PLA when $v_f > 60$ vol.-%, both the cradle-to-grave impact categories of BC-reinforced epoxy composites were found to be always higher than the cradle-to-grave impact categories of GF/PP, even at high BC loadings. This can be attributed to the production of BC, whereby the heavy environmental burden associated with the production of BC is not offset by the weight reduction of BC-reinforced epoxy composite. However, it is worth mentioning that practically, high v_f of nanocellulose within the composites could be difficult to achieve and novel manufacturing routes need to be explored. These include culturing BC in culture medium consisting of dissolved water-soluble polymers [61], co-filtering a nanocellulose suspension consisting of water-soluble polymer followed by consolidation and crosslinking [32], heat lamination of thin
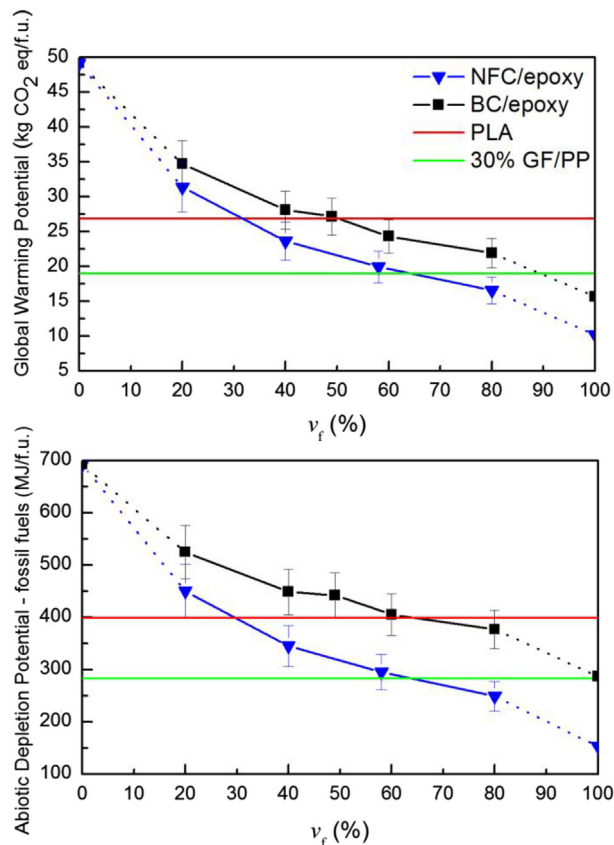
Fig. 5. GWP and ADf of the nanocellulose-reinforced polymer composites for different nanocellulose loading.

thermoplastics between nanopapers [60] and dipping of nano-papers into organic solvents containing dissolved monomer/polymer, followed by solvent evaporation and crosslinking [62].

4. Conclusions

In this work, a cradle-to-grave LCA of BC- and NFC-reinforced epoxy composites was performed to evaluate their environmental impact starting from the production of NFC or BC to the end-of-life of the nanocellulose-reinforced epoxy composites. Neat PLA and 30 wt.-% randomly oriented GF/PP were used as benchmark materials for comparison. To compare the environmental performance of materials with different mechanical performance, specific tensile moduli of the materials were used to evaluate the equivalent mass of the material required to achieve the same uniaxial tensile load. For the manufacturing phase, our study showed that BC- and NFC-reinforced epoxy composites have higher GWP (13.8 kg CO_2 eq for BC-reinforced epoxy and 8.6 kg CO_2 eq for NFC-reinforced epoxy) and ADf (271.6 MJ for BC-reinforced epoxy and 149.6 MJ for NFC-reinforced epoxy) compared to neat PLA and GF/PP even though the specific tensile moduli of the nanocellulose-reinforced epoxy composites are higher than neat PLA and GF/PP, implying that smaller equivalent mass for nanocellulose-reinforce epoxy composites is required. In addition to the production of NFC from kraft pulp (0.76 kg CO_2 eq and 28 MJ) and the biosynthesis of BC (4.8 kg CO_2 eq and 131 MJ), the composite manufacturing process, whereby numerous environmental unfriendly consumables are required for VARI, also contributes to the poor environmental performance of nanocellulose-reinforced epoxy composites.

When the use phase and end-of-life of our model nanocellulose-reinforced epoxy composites were studied, we found that neat PLA contributes to a high cradle-to-grave GWP (26.9 kg CO_2 eq) and ADf (398 MJ). GF/PP composites have the lowest cradle-to-grave GWP (18.9 kg CO_2 eq) and ADf (283.5 MJ) compared to the neat PLA. This can be attributed to the differences in the equivalent mass required between the two materials. Our LCA model further showed that when the use phase and the end-of-life of nanocellulose-reinforced epoxy composites were considered, the "green credentials" of nanocellulose-reinforced epoxy composites are comparable to that of neat PLA and GF/PP composites. Life cycle scenario analysis also showed that both the cradle-to-grave GWP and ADf of BC- and NFC-reinforced epoxy composites can be lower than that of neat PLA when $v_f > 60$ vol.-%, indicating that high nanocellulose loading fraction of composites is desired to produce materials with "greener credentials" than neat PLA. However, the GWP and ADf of BC-reinforced epoxy composites were found to be always higher than that of GF/PP, even at high BC loadings. This can be attributed to the production of BC, whereby the heavy environmental burden associated with the production of BC is not offset by the weight reduction of BC-reinforced epoxy composite. To produce "truly green" nanocellulose-reinforced polymer composites, it is therefore desirable to reduce the energy necessary for the production of NFC, synthesise BC at much higher yields and employ composite manufacturing processes with lower environmental impact.

Acknowledgement

Appendix A. Supplementary data

Supplementary data related to this article can be found at http://dx.doi.org/10.1016/j.compscitech.2015.08.024.

References

[1] A. Bismarck, C. Burgstaller, K.Y. Lee, B. Madsen, J. Mussig, C. Santulli, et al., Recent progress in natural fibre composites: selected papers from the 3rd international conference on innovative natural fibre composites for industrial applications, Ecocomp 2011 and BEPS 2011, J. Biobased Mater. Bioenergy. 6 (4) (2012) 343–345.

[2] G. Koronis, A. Silva, M. Fontul, Green composites: a review of adequate materials for automotive applications, Compos. Part B Eng. 44 (1) (2013) 120–127.

[3] K.-Y. Lee, Y. Aitomäki, L.A. Berglund, K. Oksman, A. Bismarck, On the use of nanocellulose as reinforcement in polymer matrix composites, Comp. Sci. Tech. 105 (2014) 15–27.

[4] S.J. Eichhorn, A. Dufresne, M. Aranguren, N.E. Marcovich, J.R. Capadona, S.J. Rowan, et al., Review: current international research into cellulose nanofibres and nanocomposites, J. Mater. Sci. 45 (1) (2010) 1–33.

[5] W.J. Lyons, Theoretical value of the dynamic stretch modulus of cellulose, J. Appl. Phys. 30 (5) (1959) 796–797.

[6] K. Tashiro, M. Kobayashi, Theoretical evaluation of 3-dimensional elastic-constants of native and regenerated celluloses − role of hydrogen-bonds, Polymer 32 (8) (1991) 1516–1530.

[7] K.H. Meyer, L.E.R. Picken, Natural and Synthetic High Polymers; a Textbook and Reference Book for Chemists and Biologists, Interscience Publishers, inc, New York, N.Y., 1942.

[8] F. Tanaka, T. Iwata, Estimation of the elastic modulus of cellulose crystal by molecular mechanics simulation, Cellulose 13 (5) (2006) 509–517.

[9] M. Bergenstrahle, L.A. Berglund, K. Mazeau, Thermal response in crystalline I beta cellulose: a molecular dynamics study, J. Phys. Chem. B 111 (30) (2007) 9138–9145.

[10] S.J. Eichhorn, G.R. Davies, Modelling the crystalline deformation of native and regenerated cellulose, Cellulose 13 (3) (2006) 291–307.

[11] M. Matsuo, C. Sawatari, Y. Iwai, F. Ozaki, Effect of orientation distribution and crystallinity on the measurement by X-ray-diffraction of the crystal-lattice moduli of cellulose-I and cellulose-II, Macromolecules 23 (13) (1990) 3266–3275.

[12] T. Nishino, K. Takano, K. Nakamae, Elastic modulus of the crystalline regions of cellulose polymorphs, J. Polym. Sci. Part B Polym. Phys. 33 (1995) 1647–1651.

[13] I. Sakurada, Y. Nukushina, T. Ito, Experimental determination of elastic modulus of crystalline regions in oriented polymers, J. Polym. Sci. 57 (165) (1962) 651.

[14] R. Rusli, S.J. Eichhorn, Determination of the stiffness of cellulose nanowhiskers and the fiber-matrix interface in a nanocomposite using Raman spectroscopy, Appl. Phys. Lett. 93 (3) (2008).

[15] Y.C. Hsieh, H. Yano, M. Nogi, S.J. Eichhorn, An estimation of the Young's modulus of bacterial cellulose filaments, Cellulose 15 (4) (2008) 507–513.

[16] A. Sturcova, G.R. Davies, S.J. Eichhorn, Elastic modulus and stress-transfer properties of tunicate cellulose whiskers, Biomacromolecules 6 (2) (2005) 1055–1061.

[17] J.H. de Boer, The influence of van der waals' forces and primary bonds on binding energy, strength and orientation, with special reference to some artificial resins, Trans. Faraday Soc. 32 (1) (1936) 0010–0036.

[18] R.E. Mark, Cell Wall Mechanics of Tracheids, Yale University Press, New Haven,, 1967.

[19] A.J. Stamm, E.E. Harris, Chemical Processing of Wood, Chemical Pub. Co, New York,, 1953.

[20] H. Mark, Molecular factors affecting mechanical behaviour, in: E. Ott (Ed.), Cellulose and Cellulose Derivatives, Interscience, New York, 1943, pp. 990–1015.

[21] H.P.S. Abdul Khalil, A.H. Bhat, A.F. Ireana Yusra, Green composites from sustainable cellulose nanofibrils: a review, Carbohydr. Polym. 87 (2) (2012) 963–979.

[22] S. Kalia, A. Dufresne, B.M. Cherian, B.S. Kaith, L. Avérous, J. Njuguna, et al., Cellulose-based bio- and nanocomposites: a review, Int. J. Polym. Sci. 2011 (2011) 1–35.

[23] K. Wuhrmann, A. Heuberger, K. Mühlethaler, Elektronenmikroskopische Untersuchungen an Zellulosefasern nach Behandlung mit Ultraschall, Experientia 2 (3) (1946) 105107.

[24] F.W. Herrick, R.L. Casebier, J.K. Hamilton, K.R. Sandberg, Microfibrillated cellulose: morphology and accessibility, in: A. Sarko (Ed.), Proceedings of the Ninth Cellulose Conference, vol. 37, Wiley, Syracuse, New York, 1983, pp. 797–813.

[25] A.F. Turbak, F.W. Snyder, K.R. Sandberg, Microfibrillated cellulose, a new cellulose product: properties, uses, and commercial potential, Appl. Polym. Symp. 37 (1983) 815–827.

[26] T. Taniguchi, K. Okamura, New films produced from microfibrillated natural fibres, Polym. Int. 47 (3) (1998) 291–294.

[27] K.Y. Lee, G. Buldum, A. Mantalaris, A. Bismarck, More than meets the eye in bacterial cellulose: biosynthesis, bioprocessing, and applications in advanced fiber composites, Macromol. Biosci. 14 (1) (2014) 10–32.

[28] M. Wada, T. Okano, J. Sugiyama, Allomorphs of native crystalline cellulose I evaluated by two equatorial d-spacings, J. Wood Sci. 47 (2) (2001) 124–128.

[29] K.-Y. Lee, T. Tammelin, K. Schulfter, H. Kiiskinen, J. Samela, A. Bismarck, High performance cellulose nanocomposites: comparing the reinforcing ability of bacterial cellulose and nanofibrillated cellulose, ACS Appl. Mater. Interfaces 4 (8) (2012) 4078–4086.

[30] A. Boldizar, C. Klason, J. Kubat, P. Naslund, P. Saha, Prehydrolyzed cellulose as reinforcing filler for thermoplastics, Int. J. Polym. Mater. 11 (4) (1987) 229–262.

[31] H. Yano, J. Sugiyama, A.N. Nakagaito, M. Nogi, T. Matsuura, M. Hikita, et al., Optically transparent composites reinforced with networks of bacterial nanofibers, Adv. Mater. 17 (2) (2005) 153.

[32] H. Sehaqui, Q. Zhou, L.A. Berglund, Nanostructured biocomposites of high toughness—a wood cellulose nanofiber network in ductile hydroxyethylcellulose matrix, Soft Matter 7 (16) (2011) 7342.

[33] Q. Li, S. McGinnis, C. Sydnor, A. Wong, S. Renneckar, Nanocellulose life cycle assessment, ACS Sustain. Chem. Eng. 1 (8) (2013) 919–928.

[34] C. Hohenthal, M. Ovaskainen, D. Bussini, P. Sadocco, T. Pajula, H. Lehtinen, et al., Final Assessment of Nano Enhanced New Products, VTT Technical Research Centre of Finland, 31st October 2012.

[35] E.T.H. Vink, S. Davies, J. Kolstad, The eco-profile for current Ingeo polylactide production, Ind. Biotechnol. (2010) 212–224.

[36] S.V. Joshi, L.T. Drzal, A.K. Mohanty, S. Arora, Are natural fiber composites environmentally superior to glass fiber reinforced composites? Comp. Pt A 35 (3) (2004) 371–376.

[37] H. Baumann, A.-M. Tillman, The Hitch Hiker's Guide to LCA. An Orientation in Life Cycle Assessment Methodlogy and Application. USA, 2004.

[38] S. Evangelisti, P. Lettieri, D. Borello, R. Clift, Life cycle assessment of energy from waste via anaerobic digestion: a UK case study, Waste Manag. 34 (1) (2014) 226–237.

[39] M.F. Ashby, Materials Selection in Mechanical Design, third ed., Elsevier Butterworth-Heinemann, Burlington, 2005.

[40] J. Guinee, Handbook on life cycle assessment − operational guide to the ISO standards, Int. J. Life Cycle Assess. 6 (5) (2001), 255–255.

[41] J.C. Bare, P. Hofstetter, D.W. Pennington, H.A.U. de Haes, Midpoints versus endpoints: the sacrifices and benefits, Int. J. Life Cycle Assess. 5 (6) (2000) 319–326.

[42] S. Hestrin, M. Schramm, Synthesis of Cellulose by Acetobacter-Xylinum .2. Preparation of freeze-dried cells capable of polymerizing glucose to cellulose, Biochem. J. 58 (2) (1954) 345–352.

[43] S. Josset, P. Orsolini, G. Siqueira, A. Tejado, P. Tingaut, T. Zimmermann, Energy consumption of the nanofibrillation of bleached pulp, wheat straw and

recycled newspaper through a grinding process, Nordic Pulp Pap. Res. J. 29 (1) (2014) 167—175.

[44] A.V. Marchenko, Thermo-mechanical Properties of Materials. Cold Regions Science and Marine Technology, Encyclopedia of Life Support System, Oxford, UK, 2010.

[45] Martienssen W. Polymers, in: H. Warlimont (Ed.), Springer Handbook of Condensed Matter and Materials Data, Springer, 2005, pp. 511—512.

[46] R. Le Borgne, P. Feillard, Analyse du cycle de vie — application dans l'industrie automobile, Tech. L'ingenieur (2000).

[47] A. Bignonnet, Approche globale d'allégement des véhicules, Mécanique Industries 2 (3) (2001) 173—180.

[48] S. Mudgal, L. Lyons, J. Bain, D. Dias, T. Faninger, L. Johansson, et al., European comission DG ENV: plastic waste in the environment, in: Service BI (Ed.), Institute for European Environmental Policy, 2011.

[49] P.R. Europe, How to boost plastics recycling and increase resource efficinecy? Strategy paper of plastics recyclers Europe, Plast. Recycl. Eur. (2012).

[50] J.J. Kolstad, E.T.H. Vink, B. De Wilde, L. Debeer, Assessment of anaerobic degradation of Ingeo™ polylactides under accelerated landfill conditions, Polym. Degrad. Stab. 97 (7) (2012) 1131—1141.

[51] S. Gea, C.T. Reynolds, N. Roohpour, B. Wirjosentono, N. Soykeabkaew, E. Bilotti, et al., Investigation into the structural, morphological, mechanical and thermal behaviour of bacterial cellulose after a two-step purification process, Bioresour. Technol. 102 (19) (2011) 9105—9110.

[52] J. George, K. Ramana, S. Sabapathy, A. Bawa, Physico-mechanical properties of chemically treated bacterial (Acetobacter xylinum) cellulose membrane, World J. Microbiol. Biotechnol. 21 (8—9) (2005) 1323—1327.

[53] J. George, V.A. Sajeevkumar, R. Kumar, K.V. Ramana, S.N. Sabapathy, A.S. Bawa, Enhancement of thermal stability associated with the chemical treatment of bacterial (Gluconacetobacter xylinus) cellulose, J. Appl. Polym. Sci. 108 (3) (2008) 1845—1851.

[54] A.L. Roes, E. Marsili, E. Nieuwlaar, M.K. Patel, Environmental and Cost Assessment of a Polypropylene Nanocomposite, J. Polym. Environ. 15 (3) (2007) 212—226.

[55] S.M. Lloyd, L.B. Lave, Life cycle economic and environmental implications of using nanocomposites in automobiles, Environ. Sci. Technol. 37 (15) (2003) 3458—3466.

[56] S.J. Eichhorn, Cellulose nanowhiskers: promising materials for advanced applications, Soft Matter 7 (2011) 303.

[57] M. Pietrini, L. Roes, M. Patel, E. Chiellini, Comparative life cycle studies on poly(3-hydroxybutyrate)-based composites as potential replacement for conventional petrochemical plastics, Biomacromolecules 8 (2007) 2210—2218.

[58] S. Tanpichai, F. Quero, M. Nogi, H. Yano, R.J. Young, T. Lindström, et al., Effective Young's modulus of bacterial and microfibrillated cellulose fibrils in fibrous networks, Biomacromolecules 13 (5) (2012) 1340—1349.

[59] H.L. Cox, The elasticity and strength of paper and other fibrous materials, Br. J. Appl. Phys. 3 (3) (1952) 72—79.

[60] T. Montrikittiphant, M. Tang, K.Y. Lee, C.K. Williams, A. Bismarck, Bacterial cellulose nanopaper as reinforcement for polylactide composites: renewable thermoplastic nanopapreg, Macromol. Rapid Commun. 35 (19) (2014) 1640—1645.

[61] Q. Zhou, E. Malm, H. Nilsson, P.T. Larsson, T. Iversen, L.A. Berglund, et al., Nanostructured biocomposites based on bacterial cellulosic nanofibers compartmentalized by a soft hydroxyethylcellulose matrix coating, Soft Matter 5 (21) (2009) 4124—4130.

[62] A.N. Nakagaito, H. Yano, The effect of morphological changes from pulp fiber towards nano-scale fibrillated cellulose on the mechanical properties of high-strength plant fiber based composites, Appl. Phys. A Mater. Sci. Process 78 (4) (2004) 547—552.